MICROMACHINED MID-INFRARED TUNABLE FABRY-PEROT FILTER

Norbert Neumann, Karla Hiller [1], Steffen Kurth [2]
InfraTec GmbH, Dresden, Germany
[1] Chemnitz Univ. of Technology, Center for Microtechnologies, Chemnitz, Germany
[2] Fraunhofer Institute for Reliability and Microintegration, Chemnitz, Germany
e-mail: n.neumann@infratec.de

ABSTRACT

This contribution deals with the design, fabrication and test of a micro-machined first order Fabry-Perot (FP) filter that is intended for use in advanced infrared gas analysis. To achieve optimal interference conditions within an FP filter, the roughness and the curvature of its reflectors must be minimized, while the parallelism between reflectors ~~is~~ maintained. The approach here minimizes mirror curvature by using 300µm thick mirror carriers for the coplanar fixed and movable reflectors of the FP filter. Dielectric reflectance stacks consisting of deposited alternating layers of silicon dioxide (SiO_2) and polycrystalline silicon (Si) are used as the mirror reflectors and single and a multilayer antireflection coating is used at the silicon/air interface. The cavity spacing is electrostatically driven.

Keywords: Fabry-Perot filter, Bragg reflector, Bulk micromachining, Antireflection coating,

INTRODUCTION

Pyroelectric detectors equipped with narrow band infra-red filters are widely used in infrared gas analyzers and fire and flame detection systems. The central wave-length and spectral bandwidth of the filters are selected in reference to the gases, which have to be analyzed. The more gases have to be analyzed simultaneously the more detectors, or detectors with separate spectral channels, are necessary. Flexibility and performance of a device equipped with a tunable filter are more sophisticated than a simple fixed filter approach. New measuring algorithms are possible exceptions if gas mixtures have to be analyzed in which the gases are characterized by adjacent or overlapping absorption bands. The device could be operated like a spectrometer to obtain a spectral signature. The new approach is based on a Fabry-Perot interferometer (FPI) with an air cavity, which is electrostatically tuned. The spectral region in the gas analysis application lies between 3 µm and 5 µm. The Fabry-Perot (FP) filters require extremely flat, coplanar reflectors with a very low roughness and a high reflectance to achieve a narrow bandwidth of about 50 nm, a high tuning range of at least 1000 nm, a high peak transmittance of about 70 % and an aperture of at least 4 mm^2. The transmission of a FPI is described by equation. (1), known as the Airy function:

$$I_T = \left(1-\frac{A}{(1-R)}\right)^2 \frac{1}{1+\frac{4R}{(1-R)^2}\sin^2\left(2\pi nd\frac{1}{\lambda}\cos\theta - \phi(\lambda)\right)} \qquad (1)$$

where A and R are absorptance and reflectance of the reflector, d and n the physical thickness and refractive index of the cavity gap, θ the angle of incidence, and $\phi(\lambda)$ the phase change on reflection. It can be seen from the Airy function that tuning is achieved by changing n, d or θ, and is called, respectively, refractive index tuning, mechanical tuning and spatial tuning. Mechanical tuning of the air gap, already used in the fine mechanical interferometer of Ch. Fabry and A. Perot more than hundred years ago, is also applied in modern surface micromachined solutions [1, 2]. The disadvantages of the so-called drum design are the bowing under electrostatic load of the mirror, which increases considerably the spectral bandwidth and the small aperture. Main disadvantages of the so called drum design are that the reflector bends due to the electrostatic forces used, which considerably increases the spectral bandwidth and the reduced working aperture the device. A high wavelength tuning range within a small package cannot be achieved with spatial tuning of a Bragg reflector [3], electrooptic index tuning of a liquid crystal cavity [4] or electrothermal index tuning of a germanium cavity [5] of a Fabry-Perot resonator. The electrostatically driven air cavity facilitates compact and low-power FP filters in contrast to other methods like piezoelectric actuation [6], magnetic actuation [7] or thermal actuation [8].

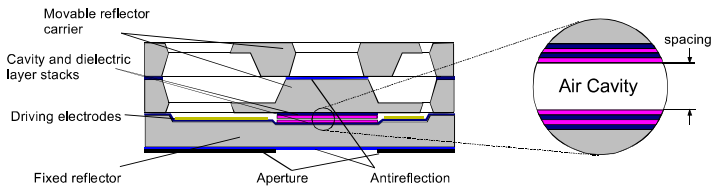

FILTER DESIGN

The FP filter is fabricated by bulk micromechanics technology to achieve optimum interference conditions. Three hundred micron thick silicon wafers with a resistivity of 5…10 Ωcm are used as the carriers for both the fixed and the movable reflector. The moving reflector, measuring 2.2 x 2.2 mm^2, is supported by a carrier, which in turn is suspended by its corners. Diagonal bending beams located in the corners elastically suspend the movable reflector. Fig. 1 shows a cross sectional view of the FP filter. The parallel spring suspension, presented in Fig. 2, results in a setup of eight diagonal bending beams that will provide the necessary vertical movement and the necessary rigidity to minimize any tilting of the movable mirror carrier [9].

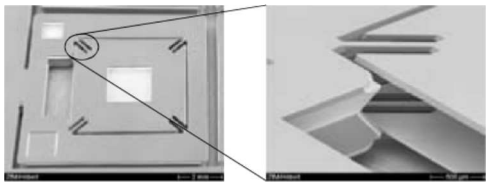

Fig. 2: SEM micrograph of the movable reflector and of the parallel spring suspension in detail

The center of gravity of the combined movable reflector carrier was designed to be in the middle plane between the two bonded wafers in order to prevent tilting by gravity. The four fixed electrodes at the topside of the fixed reflector carrier surrounding the mirror are used for electrostatic driving and capacitive detection of the cavity spacing. The electrodes are separately wired to the electronics so as to provide the opportunity to detect and compensate any tilt of the movable mirror. The outer parts of the moveable reflector carrier are used as movable electrodes. The polycrystalline silicon layers of the mirror stacks are connected to the wafers to keep these layers free of electrostatic charges. The physical distance of the reflectors and of the driving electrodes are designed for a first order tuning in the spectral range of 4…3 µm range for a short cavity filter and of 5…3 µm range for a long cavity filter.

OPTICAL DESIGN

For the Bragg reflectors an asymmetrical design $n_S |LH|^p n_0$, p = 2, 3 consisting of deposited alternating optical thickness (QWOT) layers with low and high refractive index. The low and high index material abbreviated with L and H form upon a period p. In order to generate a broad high reflective zone from 3…5 µm even with a low period number L and H layers with a high as possible refractive index ratio n_H/n_L has to apply. Silicon dioxide with a refractive index of 1.40 at 4 µm is used as low refractive index material and polycrystalline silicon with a refractive index of 3.33 at 4 µm is used as high refractive index material reflectors. The optical constants n and k were measured by an ellipsometer on QWOT layers from 2…20 µm wavelength. The layers are deposited by CVD processes and are compatible with bulk micromachining. Reflection and phase of the Bragg reflectors and the antireflection coating were computed by the matrix method and with commercial software to prove the measuring results [10].

Because of the relatively high ratio of refractive indexes n_H/n_L of 2.4 a wide high-reflective zone from 3.2…4.8 µm and a high maximum transmission of 94 % was obtained already with a $(HL)^2$ layer (Fig. 3). Increasing the number of periods to 3 increases the reflectance to 98 % and squares the high reflection zone. To reduce reflection losses and the undesirable ripples in the reflecting wavelength band caused by multiple reflections in the silicon substrate, the surface of the wafer was antireflection coated. As expected, the ripples of the in band reflectance were virtually eliminated and the reflectance was improved (Fig. 3)

The variable change in phase associated with the reflection increases the necessary deflection of the movable mirror and the driving force to tune the FPI. In the case of the $(HL)^2$ reflector this behavior is less pronounced than in the case of $(HL)^3$ reflector. Therefore $(HL)^2$ Bragg reflectors are the better choice for wide tuning FP filters from this point of view.

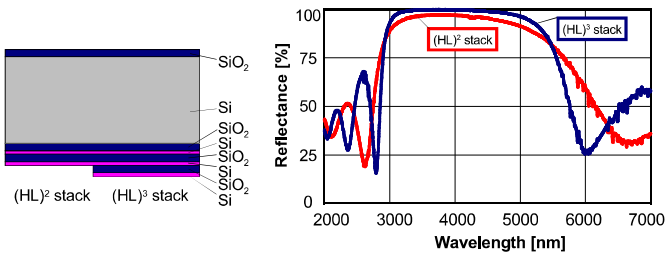

RESULTS

The optical and electromechanical design was proven on etalons with a fixed resin spacer and on tunable FP filters. On the basis of the etalons 2 and 3 periodic Bragg reflectors $(HL)^{2;3}$ and single layer and multi layer ARC specified in table 1 were tested. Thick double side polished high-resistance silicon wafer were used as reflector carriers.

Table 1: Overview of etalon types

type	reflector	ARC
V1	$(HL)^2$	$\lambda/4$-SiO_2
V2	$(HL)^2$, smooth	$\lambda/4$- SiO_2
V3	$(HL)^2$	multilayer
V5	$(HL)^2$	$\lambda/4$-Si_3N_4

A photolithographic SU-8 resin layer structure is used to adjust the air gap. The optical reference wavelength of the layer stack was adjusted to 3700 nm. The arrangement is schematically presented in Fig. 4.

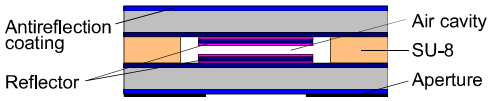

Fig. 4: Principle structure of the etalons

Great effort was taken to minimize curvature and roughness of the reflector and deposited layers and to improve the antireflection coating of the reflector carrier. The roughness of the layer stack depends strongly on the roughness of the polycrystalline silicon layer (see Fig. 5). Applying low-temperature deposited

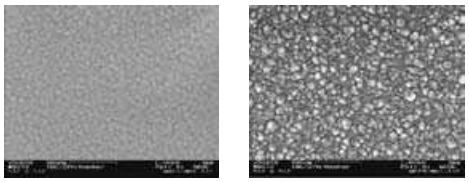

Fig. 5: Roughness of polycrystalline silicon deposited at lower and standard temperature

silicon as high refractive index material the roughness of the reflector stack has been reduced to 1.7 nm.

The results of the optical measurements presented in Fig. 6 confirm the suitability of low roughness layer stacks to achieve a transmittance of about 75 % and a spectral bandwidth of 50 nm. Broadband multilayer antireflection coating improves the transmittance in the entire spectral range of 3…5 µm and reduces the ripple caused by internal reflections in the silicon substrate. In comparison to the multilayer ARC present single ARC consisting of silicon dioxide

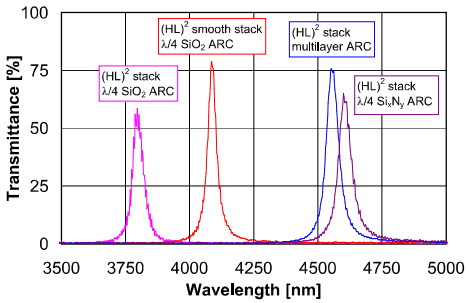

Fig. 6: Transmittance of the etalons with different Bragg reflectors and ARC

or silicon nitride a reduced performance. Transmittance measurements on single and multilayer ARC presented in Fig. 7 confirm the etalon results. The refractive index of a QWOT antireflection layer should be the square root of the refractive indices of the substrate and the incident medium:

$$n_L=(n_S n_0)^{1/2} \qquad (2)$$

The refractive index of silicon nitride of 1.9 is well matched to silicon and fulfills the equation (2) better than silicon dioxide. Therefore the insertion loss of a QWOT layer of silicon nitride is lower. Unfortunately silicon nitride layers exhibit high intrinsic stress, which produces substrate bowing after deposition, and make them unsuitable for antireflection coatings for FP filters. Alternatively a broadband multilayer ARC has a higher complexity but increases the transmittance in the whole wavelength region to at least 98 %.

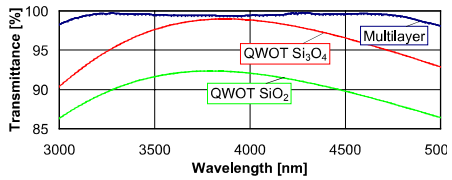

Fig. 7: Transmittance of single and multilayer antireflection coating

The tunable FP filters were designed with an optical reference wavelength of 3600 nm. Two different types have been completed. The first provides a variation of the cavity spacing between 1300 nm and 1850 nm for a tunable wavelength of 4…3 µm. The second performs a variation of the cavity spacing between 1300 nm and 2550 nm in order to cover a spectral range of 5...3 µm. $(HL)^2$ Bragg reflectors and simple QWOT SiO_2 antireflection coating were applied.

Flatness measurements were performed with an optical profiler WYKO NT1100. In Fig. 8 the deflection of the filter, the springs and the optical active area after wafer

several hundred nanometers, which is compensated by the springs. The optical active area achieve a curvature of 20…30 nm

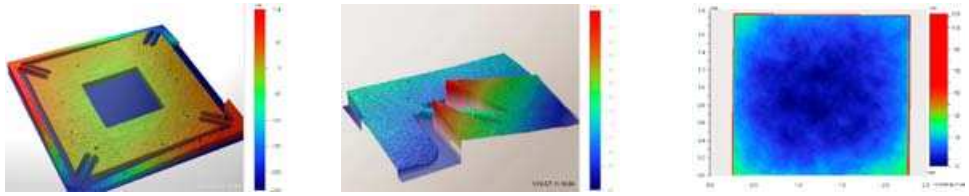

Fig 8: Flatness measurement results on FP- filter, spring and optical active area (measured by WYKO NT1100)

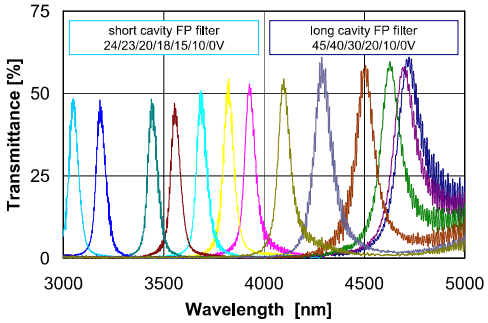

Fig 9: Spectral transmittance of short and long cavity FP filter

The spectral bandwidth of the short-cavity filter is about 60 nm and the peak transmittance about 60…50 %. The blocking of the filter is better then 0.5 %. Applying a voltage of 24 V a high tuning range from 3900 nm up to 3100 nm could be achieved (see Fig. 9). The spectral bandwidth of the long-cavity filter at the long-wavelength end is broadened, shows a high fraction of oscillations and the blocking is less compared to shorter wavelengths. It is assumed that the reason is the lower reflectance of the reflector at about 5 µm (see Fig. 3) . A narrow pass band of 50 nm bandwidth has been observed in the range of shorter wavelength

CONCLUSION

The results on fixed spacer etalons and tunable FP filters indicates that using bulk micromachining combined with thin film deposition of silicon dioxide and polycrystalline silicon high-performance filters could be fabricated. To minimize the warpage of the filter the number of wafer bonding steps should be minimized. The peak transmission can be increased further by increasing the flatness and reducing the roughness of the reflector by using low roughness polycrystalline silicon deposition and broadband $(HL)^2$ layer stack reflector is too short for a high-performance FP filter in the 3…5 µm band. To overcome this restriction two FP filters with tuning ranges from 4…3 µm and 5…4 µm and aligned optical reference wavelengths in their respective tuning range is a short-term solution. Otherwise layer stacks with an increased number of periods or an increased refractive index ratio will be tested in the next future.

Acknowledgements

This work was supported by the European Regional Development Fund 2000-2006 and by the Ministry for Economy and Labour of Saxony. The authors wish to thank Chris Varney for the helpful discussion.

Reference

[1] A. Letho, M. Blomberg, A. Torkkeli, "Electrically adjust-able optical filter", International Patent WO 98/14804
[2] M. Noro, K. Suzuki, N. Kishi, H. Hara, T. Watanabe, H. Iwaoka, "CO2/H2O gas sensor using tunable Fabry-Perot filter with wide wavelength range", Proc. Optical MEM, 319-322 (2003)
[3] G. Lammel Ph. Renaud," Free-standing, mobile 3D porous silicon microstructures", Sensors and Actuators A, **85**, 356-360 (2000)
[4] J. T. Daly, A. Bodkin, W. Schneller, R. Kerr, J. Noto, R. Haren, M. Eismann, B. Karch, "Tunable narrow-band filter for LWIR hyperspectral imaging", Proc. SPIE **3948**, 104-115 (2000),
[5] L. H. Dormash, "Thin Films sing a new tune", Photonics Spectra, **38**(11), 70-74 (2004)
[6] J. T. Knudtson, D. S. Levy, K. C. Herr, "Electronically tunable, first-order Fabry-Perot-infrared filter, Opt. Eng. **35**(8),2313-2320 (1996)
[7] H.-K. Lee, K.-S- Kim, I.-J. Cho, E. Yoon, "A wide range linearly-tunable optical filter using magnetig actuation", Proc. IEEE MEMS, 93-96 (2004)
[8] B. Hitz, Thermally actuated Fabry-Perot Filter tunes across C- and L-bands, IEEE Photonics Leters, 1894-1896, (2004)
[9] S. Kurth, K. Hiller, N. Neumann, M. Heinze, W. Dötzel, T. Geßner, "A tunable Fabry-Perot-Interferometer for 3 – 4.5 µm wavelength with bulk micromachined reflector carrier", Proc. of SPIE, **4983**, 215-226 (2003)
[10] Essential Macleod V8.9, Thin Film Center Inc., Tucson